Development of EUPS for analyzing electronic states of topmost atomic layer

— Materialization of laser-produced plasma source application and EUPS observed fascinating surface—

Toshihisa Tomie[1,2]* **and Tomoaki Ishitsuka**[2]

A quarter century has passed since the principle of EUPS (extreme UV excited photoelectron spectroscopy) was invented as the most promising application of a laser-produced plasma source. EUPS enables analysis of electronic states of the topmost atomic layer, band bending of semiconductors, estimation of carrier density, and evaluation of electrical conductivity from secondary electron signals. These newly emerged analyses provide useful information for developing catalysts, protective insulators and other materials. These new analyses were born when problems needed to be solved were brought in by users. We can say that EUPS was sophisticated by the needs of users. In this paper, we describe the historical background leading to the invention of the principle of EUPS, the selection and development of the component technologies that constitute the EUPS system, and the birth processes of novel analyses that emerged.

Keywords : Laser-Produced Plasma, EUPS, time-of-flight, topmost atomic layer, band bending, carrier density, secondary electron

1 Introduction

1.1 EUPS pioneers new applications for photoelectron spectroscopy

In 1992, extreme ultraviolet-excited photoelectron spectroscopy (EUPS) was devised as an application of laser-produced plasma (LPP) sources.[1] Since then, for a quarter of a century, we have been developing technologies for making EUPS a practical analyzing tool and pioneering applications of photoelectron spectroscopy. As we worked on gaining users to spread the use of EUPS analysis and met users' demands, new potential of EUPS were pulled out, and it became possible to conduct various analyses that are difficult or impossible with conventional photoelectron spectroscopy. It is a joy of the inventor to watch that the much wonderful potential of EUPS has become clear. The devices to be developed in the future to maintain and advance people's quality of life will require innovative functions, not just simple improvements. We expect EUPS will be one of the innovative analysis technologies that will promote technological innovations.

Currently, the EUPS system as shown in Fig. 1 is disclosed and offered for use to general users, as one of the analysis devices of AIST Nanocharacterization Facility (ANCF) which is a part of the Nanotechnology Platform Project[2] of the Ministry of Education, Culture, Sports, Science and Technology (MEXT). In this paper, we describe the process that led to the practical use of EUPS, the configuration of EUPS, and the new analysis methods pioneered by EUPS.

In Subchapter 1.2, we outline the history of LPP application research up to the creation of EUPS, and in Subchapter 1.3, the characteristic of LPP sources will be explained. The ideas for making EUPS as a practical device using an LPP source is explained in Chapter 2, the history of prototype units that led to the current working unit is described in Chapter 3, and the details of the elemental technologies that configure the current working unit will be presented in Chapter 4. The new analyses methods pioneered by EUPS will be introduced in Chapter 5.

1.2 History of the research of laser-produced plasma (LPP) sources

First, we present the history that led to the creation of EUPS that is probably the only one LPP application technology that has been put to practical use.

When a pulse laser is focused on a solid, an ultrahigh temperature state is achieved since the energy is injected before cooling by thermal conduction occurs. Several million degrees centigrade can be achieved. In such high temperature conditions, the solid becomes plasma consisting of electrons and multivalent ions. Since the density is high and the temperature is high, ultrahigh pressure is also achieved. Plasma is ejected at high speed, the solid target that is irradiated with the laser is pushed by the reaction,

1. Changchun University of Science and Technology, People's Republic of China　No.7089 Weixing Road, Changchun, Jilin 130022, China, 2. Nanoelectronics Research Institute, AIST　Tsukuba Central 2, 1-1-1 Umezono, Tsukuba 305-8568, Japan
＊ E-mail: t-tomie@aist.go.jp

and this force is usable as the propulsion of rockets in space. The idea for inertial confinement fusion, where the nuclear fusion is caused by creating an ultrahigh density condition by compressing the interior material by the reaction of exploding plasma, became realistic after the publication on laser oscillation by Maiman.[3] The paper published in *Nature* by Nuckolls *et al.*[4] in 1972 stated that there is a possibility that a breakeven, where the input energy and nuclear fusion output energy become equal, can be achieved with 1 kJ of energy, and this sent a shock around the world. Perhaps also because it was immediately after the Oil Crisis, three labs at the Electrotechnical Laboratory, which is one of the precursors of AIST, formed a group to tackle the inertial confinement fusion research. One of the authors (Tomie) was employed as one of the researchers, and was involved in the development of a high-power glass laser system for inertial fusion. In conducting the research for the glass laser oscillator, he discovered and clarified a phenomenon of pulse compression in a laser resonator.[5] This is the phenomenon of the principle of femto-second laser oscillation that emerged later. Initially, it was said that nuclear fusion was possible with a 1 kJ pulse laser, but later it was found that several MJ was necessary. The author felt that the research requiring such enormous laser power could not be continued by a small research group, and shifted the direction of his research to application of plasma using the high-energy laser he developed.

Shortly after the introduction of the laser, keV X-ray generation from LPP was observed,[6] and one calculation showed that the conversion efficiency would be comparable to X-ray tube X-ray source including the conversion efficiency from electricity to laser energy.[7] There was much research on using LPP as a high-intensity X-ray source. The author tried some approaches of application research. X-ray proximity lithography[8] was proposed as a shrink printing method of semiconductor circuits, and the development of its technology was conducted mainly using synchrotron radiation, and LPP was a candidate light source. The first LPP research conducted by the author was the use as a source of the X-ray proximity lithography. The conclusion that an X-ray reflecting mirror which can collect the X-rays irradiated almost isotopically was an essential requirement to utilize LPP as an industrial light source was the achievement of the author's research done in a very short period.

His next research was the X-ray microscopy to observe fine structures of biological cells. In living conditions, cells contain a large amount of water. By using the X-rays with wavelength range between 4.4 nm (K absorption edge of carbon) and 2.3 nm (K absorption edge of oxygen), the distribution of carbon that composes the biological cell structure, *i.e.*, the structure of a cell, can be viewed by suppressing the effect of water (oxygen). In this sense, this wavelength range is called the "water window." To observe biological cells with an electron microscope, the process of removing water is necessary, but, when the "water widow" X-rays are used, the structure of the cells can be observed in its living conditions. Much X-ray microscopy research was conducted using strong synchrotron radiation.

The reason why LPP is important as an X-ray microscopy light source is because it is an ultrahigh-intensity light source as well as a pulse source. When obtaining X-ray images by X-ray absorption, the energy density absorbed by the sample increases inversely proportional to the fourth power of spatial resolution.[9] The absorption energy density at 1 μm spatial resolution reaches several Sv (J/kg) that is a fatal dose for cells. That is, in medical diagnosis, the resolution cannot be increased too high. LPP can provide such ultrahigh-density
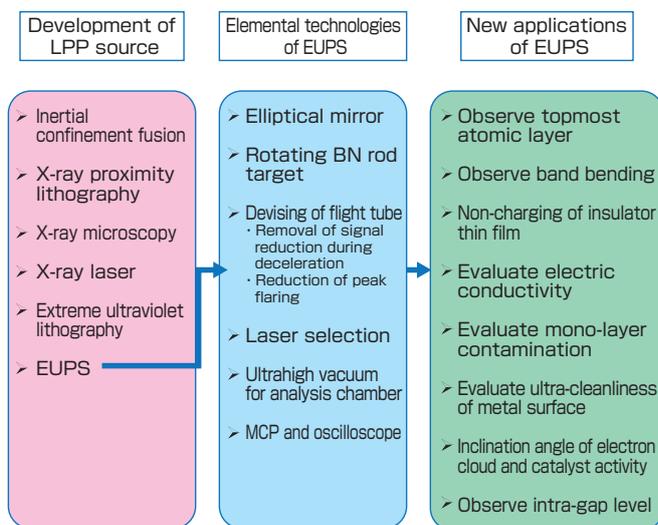
Fig. 1 EUPS Unit 2 that is available for sample analysis, and the process, configuration, and new applications of EUPS development

X-rays in an extremely short pulse of nanoseconds. At spatial resolution of several tens of nm, the necessary doze is too high and cells will instantly explode. The author *et al.* showed that a biological cell evaporated at about 60 ns using stereo X-ray photography.[10] A structure of about 50 nm was visible in the contact exposure X-ray image using LPP of a pulse width of 0.5 ns,[11] and this might have been the true structure before its destruction by thermal shock.

In LPP that has high temperature of about one million degrees and in which the electron state changes rapidly, population inversion can be generated in the vacuum ultraviolet region[12][13] and this enables the so-called "X-ray lasers." The author (Tomie) joined the X-ray laser research[14][15] team in the UK for one year in 1986, gained experience and returned home, and started research in Japan. To produce LPP for "water window" X-ray lasers, a supergiant laser system as large as we can build only one in Japan because of cost was necessary. Although it could give information of structures of living cells that was impossible with other methods, the issue was whether the use of extremely expensive giant-high-power laser system can be justified. This was also the issue faced by X-ray laser researchers around the world.

An international conference to seek the possibility of X-ray laser application to areas other than X-ray microscopy was held in the USA.[16] By reading the proceedings, the author learned of the potential of application to surface research, and stated at international conferences that the best application of X-ray lasers was to photoelectron spectroscopy.[10] The reason is because it takes the best advantage of X-ray lasers, whose greatest characteristic is extremely narrow spectrum width. In the X-ray lasers for X-ray microscopy of living cells, wavelengths outside the water window region are meaningless, high repetition rate operation of X-ray lasers is meaningless since the sample is destroyed in a single shot, and the pulse width needs to be 1 ns or less. In photoelectron spectroscopy, any wavelength can be used It is important to have a high repetition rate to obtain a large cumulative photon number in reasonably short time because decent quality spectra need large total number of detected electrons.

In the application to photoelectron spectroscopy, it is not necessary to use X-ray lasers as the light source, and an LPP source is sufficient. Moreover, downsizing is an important requirement as a practical system. The author's (Tomie) research shifted to the practical use of photoelectron spectroscopy using an LPP source from X-ray lasers, and this research is being continued to the present.

In the middle of the 1990s, extreme ultraviolet lithography (EUVL) appeared as a major application of LPP.[17] Today's information society is realized by the great progress of semiconductor technologies which was achieved by the increase of the integration by reducing the size of semiconductor circuits. This was enabled by the progress of lithography technology which prints in reduced size the circuit pattern. The progress of lithography technology was made by shortening the exposure wavelength. The shortening of the wavelength went from 248 nm of KrF lasers to 193 nm of ArF lasers, but due to the limit of the transparent wavelength of optical materials, further shortening was difficult, and a big jump of wavelength to EUV that uses reflection optics was required. The Mo/Si multilayer mirror gives a high reflectivity at 13.5 nm, and tin (Sn) LPP was selected as the source. Technologies of EUVL were developed in very big national projects in USA, Europe, and Japan. Currently, it is reported that 13.5 nm power surpassing 100 W has been obtained. Although this is an amazing figure, there is no semiconductor element made by EUVL on market yet. That is because the speed of progress of light source development failed to meet the demand of increased average power for rapid reduction of the feature size of semiconductor circuits. For the introduction to mass production plants, it is now said that several hundred watts are necessary. The author (Tomie) who was one of a few researchers working on LPP sources for X-ray microscopy was involved in EUVL since the middle of the 1990s.[17] As a person deeply involved in EUVL research for over 20 years, I hope that the increasing demand in EUV power stops and the EUVL may eventually be set for practical realization.

1.3 Characteristics of LPP source

The advantages of the LPP source[Footnote 1] include the facts that: the spectrum can be changed by selecting target material, it is short pulse, its brilliance is extremely high as shown in Fig. 2,[18] it is a point source, and others. The disadvantages are: large amount of debris contaminants (fine particles and plasma) are released as shown in the top photograph of Fig. 2, duty ratio of emission is extremely low, collection of radiation is not easy since the source emits nearly isotopically, and others.

Figure 2 shows the comparison of peak brilliance of several X-ray sources. The peak brilliance is defined by the number of photons emitted per unit solid angle per unit bandwidth per unit time from the unit surface area of the source. The data shown as black dots for LPP are values obtained in the experiments conducted by the authors, and brilliance was close to the blackbody radiation of 200-eV. This brilliance is two to three orders of magnitude larger than that of bending magnet synchrotron radiation. Compared to the X-ray tube source, LPP is 10 orders of magnitude brighter. The undulator synchrotron radiation is five orders of magnitude brighter than LPP. While the duty ratio of emission is extremely low, far lower than LPP, and the time averaged power is quite low, high-order harmonics of femtosecond lasers and X-ray lasers using LPP can have similar peak brightness to the undulator.

In the application to EUVL,[Footnote 2] the important characteristic of LPP is that it is a point source. The disadvantage of a divergent source was overcome by the development of a collecting mirror with an extremely large collecting solid angle as large as π steradian. The disadvantage of short emitting time is overcome by operating the source at high repetition rate of 10 kHz or higher.

In all LPP applications, the biggest issue is suppression of contamination of surrounding optical elements by fine particles and fast ions generated from the target. Also in the development of LPP for EUVL, the greatest obstacle for commercialization was contamination control. Historically speaking, full development of EUVL was started by the birth of an idea of using liquid Xe as a target material of LPP. Xe

atom does not stick to optics at room temperature and optics will not be contaminated.[17]

Concerning the contamination by plasma, attention is often placed only on the adhesion of atoms of the target material, but in fact, sputtering of surrounding materials by high-speed ion is more serious. In a discharge plasma source, the deterioration of electrodes by sputtering is severe. Tin is notorious as a dirty material because it adheres, but it is optimal as a material for EUVL. One of the reasons is because it is possible, in principle, to balance the adhesion of tin vapor to the surface of a multilayer reflector and the sputtering by high-speed ions. The lifetime of multilayer mirrors is extended using this principle.

2 Proposal of EUPS

2.1 Requirements of the photoelectron spectroscopy light source

As shown in Fig. 3, photoelectron spectroscopy gives information of the electronic states of a material by measuring energy of electrons released from the substance by photoexcitation. In comparison with the Auger electron spectroscopy that employs electron excitation, the good point of photoelectron spectroscopy is the high-energy resolution. In most analysis, resolution of about 1-eV is sufficient. Ordinary resolution XPS[Footnote 3] widely used in material analysis is 0.8-eV, and it is 0.3-eV in high-resolution XPS. Incidentally, resolution of 0.3-eV is confirmed for EUPS.

To obtain a photoelectron spectrum with high energy resolution, an excitation source should have a narrow bandwidth and an electron spectrometer needs to have a

Fig. 2 [Top] Photograph of LPP. Greatest issue for practical application is stopping debris contamination. [Bottom] Comparison of peak intensity of various sources.[18]
LPP is a source with intensity 2–3 orders of magnitude higher than bending magnet synchrotron radiation and nearly 10 times higher than X-ray tube. However, emission time is as short as several nanoseconds, and the time-average power is extremely low without clever ideas

Fig. 3 Principle of photoelectron spectroscopy
Because the best characteristic of photoelectron spectroscopy is high energy resolution, narrow bandwidth of the excitation light and high energy resolution of electron spectroscopy are required.

high-energy resolution. To reduce statistical noise, large cumulative counts are necessary.

The research of photoelectron spectroscopy using LPP as an excitation source was conducted by a different group,[19] and the accumulation time needed to obtain photoelectron spectra was extremely long. If the laser pulse width is 10 ns and the emission time is the same, duty ratio of emission is only one ten-millionth of the time when repetition rate is 10 Hz. Even if a laser can be operated at 1 kHz the emission duty ratio is one hundred-thousandth. As seen in Fig. 2, even if the instantaneous peak brilliance of LPP is extremely high, the time averaged photon flux is low. The response we received when we presented the principle of EUPS at an academic society was "LPP would never be a practical source for practical photoelectron spectroscopy."

2.2 Devising the EUPS

In EUPS, we overcame the disadvantage of LPP that the duty ratio is small by two ideas. One was not to use a spectrometer to obtain a narrow bandwidth light for excitation. The other was to use the time-of-flight (TOF) method for analyzing electron energy.

In a synchrotron radiation facility, the photon flux on the sample is considerably lower than the flux of the source. The reason is that the transmission of a diffraction grating spectrometer to obtain a narrow bandwidth light from the continuous spectrum light is extremely low, and the light intensity decreases by four to five orders of magnitude by passing through the spectrometer. With an LPP, a narrow bandwidth line can be generated by appropriate selection of target material and laser irradiation conditions. Although a single line spectrum cannot be obtained, as shown in Fig. 4, almost a single narrow bandwidth line spectrum can be selected using an appropriate filter. Since this eliminates a spectrometer, photon flux on sample at 10 Hz repetition rate can be comparable to that in a synchrotron facility.[18]

The use of TOF electron energy analysis changes the short pulse nature of LPP from a disadvantage to a big advantage.

In TOF, as shown in Fig. 5, the electrons produced in a short pulse fly a certain distance, are detected by detectors with a high temporal resolution, and the velocity distribution of electrons is recorded.

When the electrons are produced continuously in time, the energy of electrons is measured using the fact that the degree of bending of the trajectory of electrons by an electric field differs per the speed of electrons. The electric field is applied between the electrodes having double hemisphere or a double cylinder structure. Multiple electron detectors can be placed to detect electrons having different energies, but basically, only the electrons with one specific energy are detected. Therefore, the detection efficiency is extremely low, because all other energy electrons are not detected and thrown away. On the other hand, in TOF, electrons of all energies are detected in one measurement, and the detection efficiency is high. In principle, 100 % detection efficiency is possible in TOF. To suppress the radiation damage of material by inner shell excitation that is thought to occur after 10,000 excitations of one atom, high detection efficiency is absolutely important.[18] If the efficiency of collecting electrons is high, the excitation intensity of the sample is reduced, and then, the employment of the TOF method is effective also to suppress charging when observing insulators.

Being a pulse source was considered a disadvantage of LPP since the duty ratio is low, but as explained above, it is, in fact, an important advantage in the application to photoelectron spectroscopy since the TOF method having a high detection efficiency can be utilized. There were works of research on TOF electron spectroscopy using high-order harmonics of femtosecond laser pulses as an excitation source,[20] but EUPS is the first to utilize TOF with LPP as a light source.
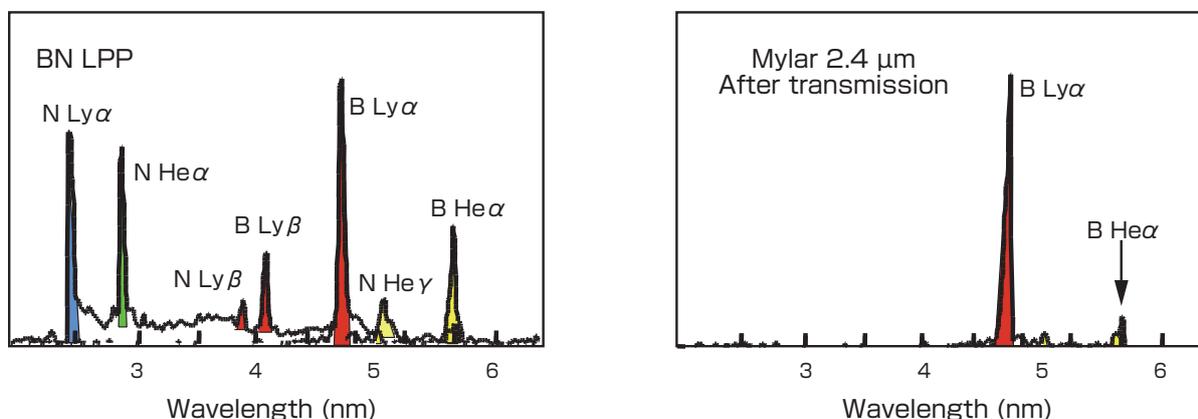
Fig. 4 LPP source spectra used in the EUPS[21]
The emission spectrum of boron nitride LPP (left) becomes almost monochromatic (4.86 nm) after passing through a Mylar film (right). Spectral loss for obtaining a narrow line is very small

3 History of the EUPS prototypes

The basic principle of EUPS is described in the patent,[1] but development and advancement of several elemental technologies were necessary for making it a practical analyzing tool.

The target material of LPP for EUPS is uniquely determined. As mentioned above, the biggest issue in any LPP application is the shielding against contaminants. In photoelectron spectroscopy, it is necessary to avoid contamination of even a mono atomic layer on the sample surface, and the use of a filter that completely shields from all substances emanating from the plasma is mandatory. Since EUV light must pass, the first requirement is that the filter must be ultrathin. On the other hand, since it must block fast ions and fine particles, the second requirement is that the filter must have certain mechanical strength with certain thickness. The filter is contaminated and damaged by ions and debris from a target, and the filter must be exchanged frequently. Therefore, the third requirement is that the filter must be low in cost. In practical use, this is extremely important.

As a material fulfilling these three requirements, we selected a carbon polymer film. Mylar, which is also a product name, can be purchased as a film of thickness of 1.4 μm at a reasonably low price.

Light of wavelengths near the long wavelength side of the K absorption edge of 4.4-nm of carbon can pass through a Mylar film at high transmissivity. The wavelength of the Lyman α line of hydrogen-like boron ions is 4.86-nm and is very compatible with Mylar. There are other emission lines emitted from a boron plasma, but they are absorbed strongly by a Mylar filter, and their intensities are negligible in practice. Boron nitride (BN) including boron can be purchased in a shape of rods. The emission of nitrogen

plasma is at the short wavelength side of the K absorption edge of carbon, and it is largely absorbed by the Mylar film and does not greatly affect the photoelectron spectrum measurement.

The fact that a boron plasma emits a strong line in the wavelength region that can pass through an inexpensive Mylar film of sufficient thinness, and boron is supplied in a rod form at a reasonable price was a gift from god to us for the realization of EUPS.

To clearly state that our photoelectron spectroscopy is different from conventional ones, in 2001, we named our scheme as "EUPS" after extreme-ultraviolet-excited-photoelectron spectroscopy.

3.1 Prototype 1

The development of EUPS was started from the middle of the 1990s. In the prototype Unit 1 for the verification experiment of the basic principle, the sample to be measured was placed in a magnetic shielded flight tube of 50-cm length, a target for LPP was placed close at a few cm, and plasma was produced by focusing a pulse laser on the target.[21] The pulse energy was 100-mJ. A BN plate was used as the target material, a Mylar thin film was sandwiched in a very narrow space between the sample and the plasma, Lyman α line emission of the hydrogen-like boron ion was selected by the Mylar filter. Photoelectrons from Si2p with the kinetic energy of about 150-eV was slowed down to about 15-eV by applying about 135-V to the flight tube, hence the flight time was lengthened by reducing the speed to increase the energy resolution that was limited by time resolution. Chemical shifts of Si2P electrons in the Si substrate, SiO_2, and SiN films were observed separately in photoelectron spectra obtained by summing up the time waveforms of 96 shots,[22] Thus the principle of EUPS was confirmed. The Mylar film worked as a vacuum separator, and the vacuum of the plasma space was about 10^{-3} Pa and the
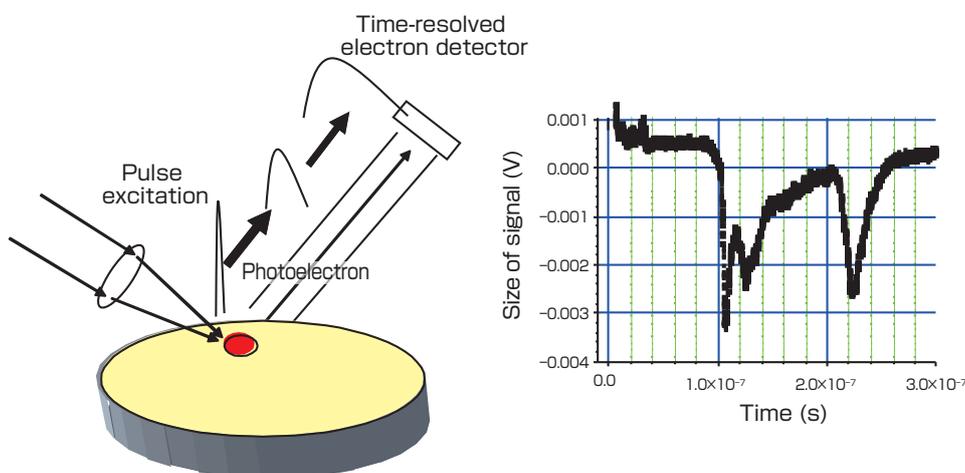
Fig. 5 Detection efficiency of TOF energy analysis is very high since particles of all energies can be detected simultaneously

vacuum of the sample space was about 10^{-4} Pa.

Through the experience with Unit 1, we could extract the issues to be solved for the realization of EUPS. The hardest thing in operating Unit 1 was the exchange of Mylar films used for wavelength selection and vacuum separation. In the Unit 1, it was necessary to set the LPP close to the sample to not weaken the EUV intensity on the sample. The Mylar film then became quickly contaminated with the debris from the target and had to be exchanged after a short time operation. Moreover, since the space between the sample and the plasma was very narrow, the exchange of the Mylar film was extremely difficult.

3.2 Unit 3 and Unit 4

After the experience with Unit 1, we fabricated Unit 2 that is currently in operation. The elemental technologies were improved as explained in the following chapters, and the current unit does not have any elements of the first Unit 2, but the basic configuration is unchanged. The prototype units with different configuration from Unit 2 were also fabricated, and we shall first describe them briefly.

In Unit 3, the efficacy of the magnetic bottle[Term 1] was investigated as it was expected to increase the capture efficiency of the electrons. The expected performance was not obtained and we decided not to adopt a magnetic bottle.

In Unit 4, the spatial resolution was pursued. Using a Schwarzschild collector optics,[Term 2] submicron beams were formed, and we succeeded in obtaining photoelectron images with a spatial resolution of less than 1 micrometer

On the surface of the convex and concave mirrors that configure a Schwarzschild mirror, it is necessary to form a multilayer film to have a high normal-incidence reflectivity. The peak reflection wavelength is at a slightly long wavelength side of 13-nm in the case of Mo/Si. Wavelength close to 6.7-nm of the La/B4C multilayer film can be also employed as an excitation light although the multilayer technology is not so mature for Mo/Si. Since it is difficult to emit an isolated, strong line emission at these wavelengths, the energy resolution of photoelectron spectra is not high when using Schwarzschild optics. Also, the collected solid angle of the source emission is small, the photon number on sample per shot is small, and a high repetition rate over 10-kHz is necessary for the source to attain a practical measurement speed. In the range that we conducted the survey, we could not find strong demands that matched the difficulty of the technology for spatial resolution of one micron. So, we stopped the development of the system using a Schwarzschild collector mirror.

4 Elemental technologies that configure the working unit

The EUPS Unit 2 was designed following the experiences gained from Unit 1, and it is currently in operation. There were three major changes from Unit 1. One was to insert an elliptical mirror between the sample and the plasma. Second was that the form of the target for LPP was changed from a plate to a rod. Third was to set the flight tube vertically. The schematic configuration of Unit 2 is shown in Fig. 6.

4.1 Use of elliptical collecting mirror

In a practical photoelectron spectroscopy system, continuous operation over a long time is mandatory. This is an extremely difficult requirement in the application of LPP that releases large amount of contaminants. It is necessary to dramatically reduce the deposition rate of contamination on the film used for vacuum separation. The primary method is to increase the distance between the plasma and the vacuum separation film.

Therefore, we used a configuration where the image of the plasma is transferred to the sample using an elliptical mirror with a long axis length of 70-cm. Since sufficient space was made between the elliptical mirror and the plasma, the Mylar film was set at 10-cm from the plasma. After some devising, currently, measurements can be done without exchanging the Mylar film for about one week.

To increase the reflectivity of 4.86-nm light, a Ni/C multilayer film was formed on the elliptical mirror, and the design value is peak reflectivity of 25 % with a bandwidth of 0.5-nm.

4.2 A rotating BN rod target

When the plasma is produced by focusing a pulse laser on solids, the area is heated to high temperature and blows off and a hole of several tens of microns diameter is formed. When the laser is focused on the hole, the density of the produced plasma is low and the emission intensity decreases greatly. To maintain the emission intensity, it is necessary to focus the laser on a flat surface. In Unit 1, the position of a BN plate was scanned for generating LPP on a flat surface, but since the scanning mechanism of the plate was complex and a large space was necessary, the form of the target was
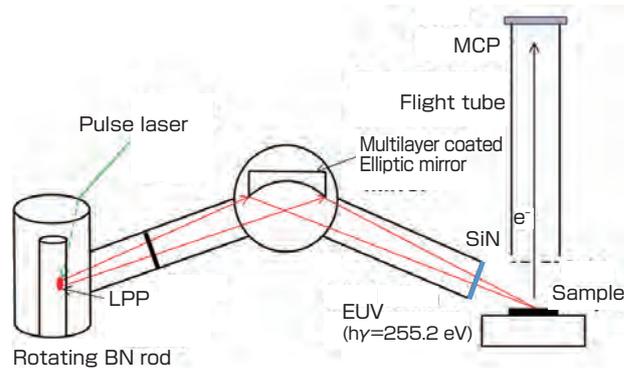
Fig. 6 Configuration of EUPS Unit 2

changed to a rod in Unit 2. In Unit 2, by rotating and moving a rod up and down (spiral motion), one rod is now employed for about one week without exchange.

4.3 Devising on the flight tube

The flight tube set horizontally in Unit 1 is set vertically in Unit 2, which allows setting a sample horizontally. By setting the sample holder horizontally, transferring a sample from the load-lock chamber to the analysis chamber became easy. The manipulator that holds a sample has five degrees of freedom, and as will be explained in Subchapter 5.6, the angle of incidence of 4.86-nm light on the sample can be changed. In ordinary EUPS measurement, in order to increase the photoelectron signal, the angle of incidence is set at 10 degrees from horizontal.

When the mass of electrons is set as m_e and the kinetic energy as E, the velocity v is $v = (2E/m_e)^{1/2}$, and the time of flight t when flight distance is L is $t = L(m_e/2E)^{1/2}$. The speed of electrons with the kinetic energy of 100-eV is 6×10^8 cm/sec, and when the flight distance is $L = 48$-cm, the time of flight is $t = 80$-ns.

The energy resolution ΔE when time resolution is Δt is
$$\Delta E = -2(\Delta t/t)E \propto \Delta t E^{3/2}$$
and when the time resolution is $\Delta t = 3$-ns, the energy resolution for 100-eV electrons is $\Delta E = 2 \times 100 \times 3/80 = 7.5$-eV. This is insufficient for photoelectron spectroscopy. If 100-eV electron is decelerated to 10-eV, the energy resolution is $\Delta E = 0.24$-eV that is sufficiently high in energy resolution. To obtain high energy resolution, the electron is slowed down in TOF. If the sample is grounded, by setting the potential of the flight tube at −90-V, the 100-eV electron is decelerated to 10-eV.

The energy resolution increases by decelerating the electrons, but we faced a problem that the signal decreased when the electrons decelerated. Also, it was found that the low energy side of the peak flared out to disfigure the waveform. These problems that inhibited the obtainment of a good photoelectron spectrum were solved by the two patented methods.

4.3.1 Solving the problem of reduced signals when electrons are decelerated

The reason the signals decreased when the electrons were decelerated was considered to be that the electrons heading for the MCP detector would go toward the wall (and therefore the solid angle detected by a detector would become small), because the speed in the direction toward the wall did not change while the speed heading for the MCP[Term 3] detector was greatly suppressed. To solve this problem, we fabricated decelerating electrodes having a curvature, as shown in Fig. 7.[23] If electrons are generated at the center of the curvature, the direction of the motion of electrons will not change by deceleration, the collecting solid angle of the detector will

not change, and the signal intensity will not change. If the electron source is set outside the curvature center, due to the retarding electric field, the velocity component heading to the cylinder wall will further decelerate, enabling "convex lens effect" that bends the electrons to the center direction of the cylinder, and thereby the signal becomes larger.

4.3.2 Solving the problem of the flaring peak

The other problem was that a large slowly decaying signal accompanied after a peak which should decay sharply. The origin of this signal was unknown for several years, but through some experiments we identified it as originating from the flight tube wall.

The photoelectrons emitted from a photo-irradiated sample are released at wide angles. Some of the electrons directly arrive at the MCP detector, while the majority of the electrons hit the flight tube wall. Then, new secondary electrons with low energy are emitted from the flight tube wall. Since the secondary electrons have low speed, they reach the MCP after the photoelectrons are directly captured by the MCP from the sample. The secondary electrons generated from the flight tube wall are also released with wide angular distribution, and the fraction of secondary electrons that arrive at MCP is high if they come from the flight tube wall close to the MCP, and is low as the distance increases. The arrival is delayed as the distance is further away from the MCP. This is the origin of the component that gradually decays after the peak. We made such an inference.
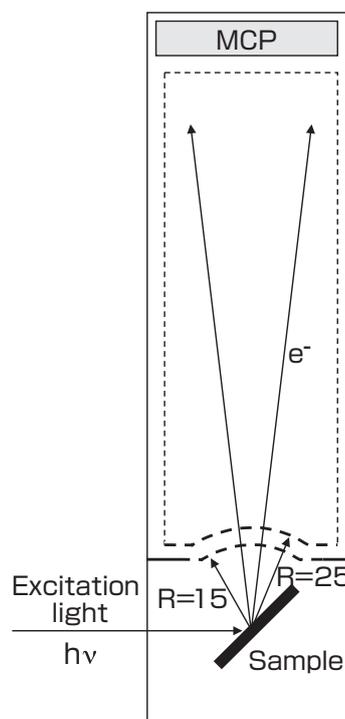
Fig. 7 Curvature is given to the decelerating electrodes to solve the problem where the signal decreases when decelerating electrons for high-energy resolution[23]

From the above consideration, we devised a way to prevent the secondary electrons from the flight tube wall to arrive at the MCP, as shown in Fig. 8.[24] Several collars were set near the exit of the flight tube near the detector, so the photoelectrons released from the sample were not blocked but the secondary electrons from the flight tube wall could not reach the MCP. The second idea was to use a mesh as the flight tube wall rather than a plate. By increasing the opening ratio of the mesh, the number of secondary electrons generated from the wall mesh is greatly reduced. Since the mesh line has a curvature, most of the secondary electrons generated at the wall mesh would not go to the MCP. By these two ideas, the large flare after the peak was reduced and became negligibly small.

4.4 Selection of a laser

As a laser for production of LPP, a laser named Infinity from Coherent, Inc. is employed. Special feature of Infinity is the use of a stimulated Brillouin scattering (SBS) mirror.[Term 4] The SBS mirror enables good Gaussian beam profile with a pulse width of 3 ns, for a very wide range of pulse energy and a repetition rate up to 100-Hz. These are extremely important characteristic of a laser for scientific experiments, particularly for EUPS.

The Q-switch YAG laser used in Unit 1 is one of widely-used lasers. Since it was not equipped with an SBS mirror, the time and spatial waveform of the laser beam change when the repetition rate or pulse energy is changed and operation at constant output power is required. The pulse width was about 10 ns, and a pulse of 2.5-ns was obtained by devising electric pulses of the Q-switch, but small pulses were present on both sides and was not a single Gaussian. With the YAG laser in Unit 1, the pulse energy of about 100-mJ was necessary to obtain the same EUV intensity obtained by Infinity operated
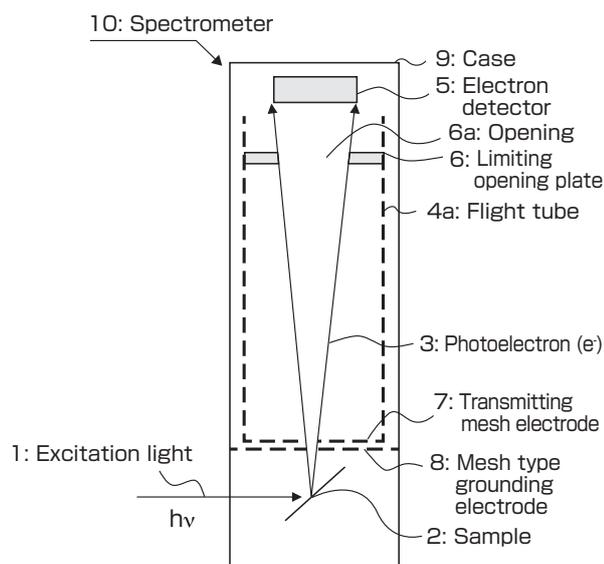
at 30-mJ. The production of contaminant substances from the target is nearly proportional to the pulse energy, and the speed of contamination of the Mylar film increases. From the point of safety, use of second harmonic of 532-nm wavelength is the same as for Unit 1.

4.5 Ultrahigh vacuum for the analysis chamber using a SiN filter of thickness of 100-nm

The vacuum separation of the LPP space and the elliptical mirror space is done using a Mylar film, but the degree of vacuum separation by the Mylar film is about six orders of magnitude, and the degree of vacuum in the elliptical mirror space remains at 10^{-4} Pa. The Mylar film deteriorates due to exposure to plasma, and the degree of vacuum separation decreases. The Mylar film is exchanged when the elliptical mirror space reaches 10^{-2} Pa.

To keep 10^{-7} Pa for the analysis chamber even when the elliptical mirror chamber reaches 10^{-2} Pa, the elliptical mirror space and the analysis chamber are vacuum separated by using a SiN film. Since the absorption coefficient of SiN film at 4.86-nm is large, to reduce the intensity drop of EUV light by the SiN filter, the SiN film of thickness of 100-nm or 50-nm is employed. The transmission at 4.86-nm are 17 % for a 3-μm Mylar and 48 % for a 100-nm SiN. Since the reflectivity of a NiC multilayer film of the elliptical mirror is 25 %, the total transmission is calculated as 2 %.

4.6 MCP and oscilloscope

In TOF energy analysis, the time resolution limits the energy resolution. Therefore, high time resolution is required for the MCP that detects the electrons and the oscilloscope that records the electron current. Products with about 1-ns time resolution were selected for the two components. To obtain large signals, it is necessary to have a large solid angle for electron capture, and MCP with a diameter of 40-mm is selected. To the author's knowledge, it was the largest commercially available product.

Since the time interval of detected electrons is long in an ordinary photoelectron spectroscopy, counting detectors with several μs dead time can be used. In EUPS, however, dozens of photoelectrons arrive in 200-ns and several tens of thousands of secondary electrons in 3-μs time, so, conventional counting detectors cannot be used. In EUPS, electrons are detected as an electric current recorded by using an oscilloscope. To reduce memory size, an average of signals of several tens to several hundred shots is calculated in the oscilloscope.

4.7 Event counting mode

Recently, we have more cases to measure very small photoelectron signals. The major problem we encountered when measuring very small signals was that good spectral waveforms were not obtained even by increasing the number

Fig. 8 Method for reducing the noise originating from flight tube wall[24]

10: Spectrometer
9: Case
5: Electron detector
6a: Opening
6: Limiting opening plate
4a: Flight tube
3: Photoelectron (e⁻)
7: Transmitting mesh electrode
1: Excitation light
hν
8: Mesh type grounding electrode
2: Sample

of accumulating shots.

We thought the cause was the electric noise in the signal systems such as in the cables and the oscilloscope interior. Since the amplification of the MCP detector is very large, one electron signal is larger than the electric noise. However, the probability of arrival of electrons at a specific time in many shots is extremely low. On the other hand, the noise appears at the same time position in every shot. Therefore, when the signals of multiple shots are averaged, the electron signal is buried in the noise. This problem can be solved by recording TOF signals of all shots without averaging, and removing the noise from each shot signal.

The oscilloscope we selected has the sequential mode. In this mode, all signals of 1-μs duration with the 0.1-ns sampling interval can be recorded at 10–50 Hz repetition rate. Recently, the small signals are often recorded in the sequential mode. However, it is limited to a special purpose, because the data volume in one measurement is enormous, and consumes a large capacity of the data server.

A signal above a certain level is set as one event. Event counting is expected to remove all electric noise. By adopting this counting mode, it has become possible to observe ultra-weak structures as presented in Subchapter 5.7.

5 Pioneering of new photoelectron spectroscopy method using EUPS—Users' demand advanced the device

EUPS is the only one device in the world. But we were aware that it will not be widely used by people simply because it is the only one in the world. We were aware that general users would not use this device unless we became the user and demonstrated findings observable only by EUPS. Therefore, after the system technology was also completed, we embarked on using the EUPS to observe various samples for the following 10 years.

However, we did not imagine that we ourselves had not rightly evaluated the EUPS that we created. The potential of EUPS was brought forth in the process of our contacting many users, the users contacting us, and solving many problems that the users brought to us to solve. We can say that EUPS was advanced by the users. New analysis methods were born from the users' demands, and the system was improved. This relationship is shown in Fig. 9.

EUPS is capable of the following analyses that are impossible or difficult using the conventional photoelectron spectroscopy[25]:

1. Analysis of the electronic states of the topmost atomic layer
2. Evaluation of band bending in semiconductors
3. Analysis of insulating films without charge neutralization
4. Evaluation of cleanliness of nanoparticle metal surfaces
5. Evaluation of electric conductivity of nanoparticle surfaces
6. Evaluation of the inclination angle of electron clouds

5.1 Observation of the topmost atomic layer
When we initially started the development of the EUPS technology, many people commented that a wavelength of 4.86-nm is too long, and that the fact that 1s electron of carbon and oxygen and deep inner shell electrons of various elements cannot be excited was a serious deficiency as photoelectron spectroscopy. We replied that inner shells other than C, N, and F could be seen with 255-eV photon energy. But at that time, we did not realize that 4.86-nm was indeed the best wavelength before we started analyses of various samples.

The first sample observed by EUPS was a Si wafer. Only Si2p of the natural oxide layer on the surface was observed and Si2p of the substrate was not observed. The Si2p of the substrate was observed only after hydrofluoric acid treatment and Si2p of the oxide did not disappear easily. There were comments that EUPS observes only contaminations which we do not want to see. However, this was an ugly duckling. The very large signals of contaminations that normally could not be observed in conventional spectroscopy turned out to be extremely useful in surface analysis.

Figure 10 shows an example of contamination analysis conducted by researchers of Panasonic Corporation.[26]

To improve the performance of the insulating protection film on electrodes in a plasma display, Panasonic researchers were trying to improve the manufacturing process by reducing contamination. Previously, they evaluated the contamination of the insulation protection film by XPS, but the signal originating from contamination was very small. At an exhibition for analyzing devices, they knew EUPS, came to us and confirmed the sensitivity of EUPS by evaluating a sample. They conducted a joint research project with us. Figure 10 is the comparison when seeing the same sample using XPS and EUPS. Clearly EUPS has higher sensitivity. They evaluated contamination of the insulating film produced in various processes. We received a report that the actual manufacturing processes were improved based on the results of EUPS analysis.

The EUPS spectrum of a sample supplied by an AIST

Development of device

Development of evaluation method ← Problem solution for users at industries
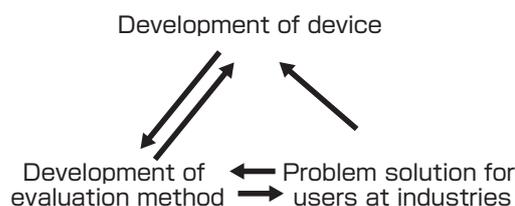
Fig. 9 Process of EUPS advancement

researcher is shown in Fig. 11. The Si2p signal of the substrate can be observed by removing the natural oxide film on the surface of a Si wafer by hydrofluoric acid treatment. In a sample with SiO_2 of thickness of 2.1 nm, substrate signal was only 10 % of that in the cleaned sample, and was hardly seen through a SiO_2 film of 4.9-nm thickness. This tells that about 0.5-nm from the surface is observed in EUPS. On the other hand, we know XPS observes an average of several nm depth from the fact that the substrate signal is greater for a SiO_2 film of 2-nm thickness.

The difference in depth resolution of XPS and EUPS is due to the difference in kinetic energy of observed photoelectrons. The "escape depth," which is defined as a depth that the electrons escape into the vacuum without losing energy in materials, has very small dependence on materials and it is smallest at the kinetic energy of several tens to a hundred eV, and it is about 0.5-nm.[27] When observed by XPS, the kinetic energy of a Si2p electron is larger than 1-keV, and the escape depth is several nm. Figure 12 shows the escape depth observed by EUPS.[28] When the kinetic energy of the electrons decreases, the escape depth increases rapidly in insulators.

At the time when we invented the principle, we had no knowledge that the photon energy at around 200-eV used in EUPS was optimal for obtaining information of the topmost atomic layer.

5.2 Observation of band bending in semiconductors

The Si wafer was selected as the first sample of photoelectron spectroscopy using EUPS, to see whether the n-type and p-type could be distinguished. It was found that the peak positions of Si2p differed in n- and p-types but they did not agree with the difference of the Fermi level of different doping.[Term 5] Also, we noticed that the peak positions changed
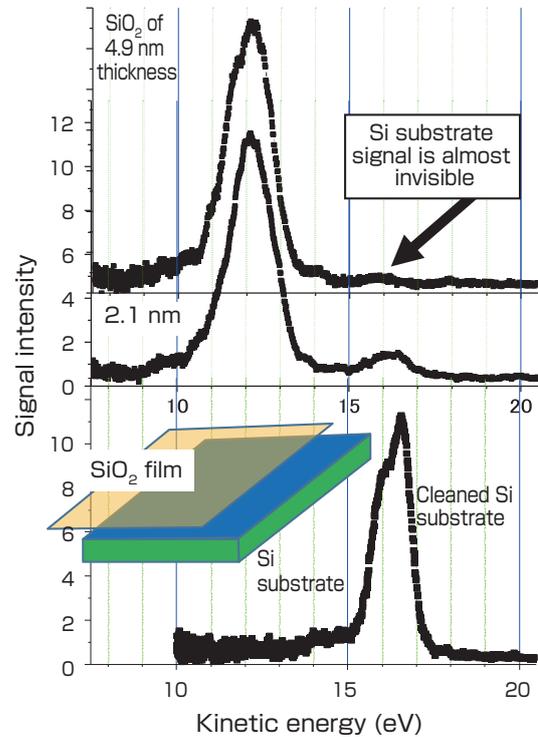
Fig. 11 Depth resolution of EUPS was evaluated to be about 0.5 nm, from the size of the background signal seen through a SiO_2 film of thickness of 2.1 nm

Single atom layer is about 0.3 nm, and information for the topmost atom layer can be obtained.

Fig. 10 Comparison of the sensitivity of EUPS and XPS in the contamination analysis for improving production process of insulator film protecting electrode in a plasma display[26]
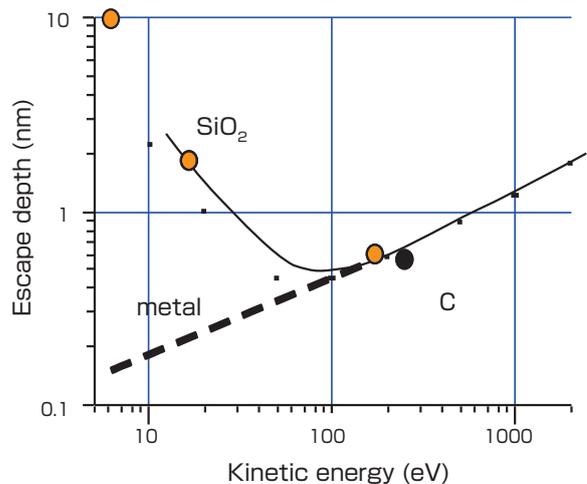
Fig. 12 Kinetic energy dependence of escape depth of electrons was investigated by EUPS[28]

Material dependence is large at the energy of 100-eV or less, and there is no "universal" curve.

– 223 –

when the irradiation intensities were changed. It took a few years for us to understand that the observed phenomenon was related with band bending.[Term 6] This phenomenon occurred by the flattening of the bent band. With other sources bent band cannot be flattened, but it is possible with EUPS where ultrahigh density pulse excitation is used.

When an HfO_2 film with thickness of 12-nm formed on a Si wafer was measured by EUPS, the position of the Hf4f peak was dependent on the excitation intensity of EUV. When the measurement at strong excitation was continued, the peak position shifted to the low kinetic energy side. After the shift was saturated and the measurement was taken at different intensity, the intensity dependent peak shift increased further.[29]

When positive charge is captured in an insulating film, the potential of the electrons on the Si surface lowers because of the electric field generated by holes, and the peak of the photoelectron spectrum shifts to the low kinetic energy side. The captured positive charge increases for larger EUV irradiation, and then, the charge shift increases. When all the charge trapping centers are filled with the charges, the charge shift stops.

When the sample is photo-excited, the electron-hole pair is formed in the sample. Due to the electric field created by the charges in the insulation film, the electrons flow to the insulation film/Si interface while the holes flow to the Si interior. The electric field created by the separated electrons and holes offsets the electric field created by the charges captured in the insulating film on the surface. If a sufficiently large number of electron-hole pairs is created by increasing the excitation intensity, it is possible to completely cancel out the electric field created by the charges in the insulating film. That is, the bent band can be totally flattened.

When the surface density of the charges captured in the insulation film is set as $10^{12}/cm^2$, the electron-hole pair of a similar density or higher is needed for a flat band. Assuming the lifetime of an electron-hole pair as 10-ns, it is necessary to create an electron-hole pair at $10^{20}/(cm^2\ sec)$. However, the most powerful light emission facility in Japan, that is the hard X-ray undulator of SPring-8 in Himeji, has a photon flux of only 2×10^{16} photons/(cm^2 sec), and cannot affect band bending to a detectable level. On the other hand, in EUPS, the photon density on a sample per pulse is estimated to be 3 $\times 10^{12}/cm^2$, and if 10 or more electron-hole pairs are produced for one 255-eV photon, it is possible to flatten the band bending produced by a charge of about $3 \times 10^{13}/cm^2$.

Evaluation of band bending is an important analysis characterizing semiconductors, and it is possible with an ultrahigh intensity pulse source as explained above. We could never have thought of this when we invented the EUPS.

5.3 Insulating film is not charged

In XPS, the electrostatic charge in the insulating material is a major problem. We knew that it was almost mandatory to install a neutralizer gun to neutralize the charge in photoelectron spectroscopy, but a neutralizer is not installed in the EUPS Unit 2. As the electrostatic charge in the insulating material was our concern, we studied SiO_2 ultrathin films and found they were not highly charged.

When a thermal oxide film of thickness of 100-nm was observed, the Si2p shifted with time, but it saturated with a shift of about 3-eV. It was then fully charged by irradiating the ion beam with a very small current. When this charged sample was EUPS measured, the peak shift was about 25-eV initially but peak shift decreased rapidly and the decrease of the shift stopped at a shift of about 10-eV. Next, after heating the sample to nearly 1000 ℃ by using infrared rays, EUPS measurements were done and it was found that the charge had almost entirely disappeared. As the EUPS measurement was continued the charge shift was noticed, but it was only 0.1-eV.[30]

Textbooks of photoelectron spectroscopy explain that an insulating film is charged by photoexcitation because holes left after electrons are released into the vacuum do not flow through the insulating film to the substrate metal. We know this explanation is not correct from the result seen in Fig. 13. The result in Fig. 13 can be explained as follows.

Since a charge shift of 25-eV was observed with ion irradiation, we know that the SiO_2 used in the experiment had a high dielectric strength (>4 MV/cm). Since the charge shift decreased by EUPS measurement, it can be understood that EUV irradiation decreased the dielectric strength of SiO_2. It can be explained that the electron-hole pairs are created by EUV irradiation, this gives conductivity to the insulating film,
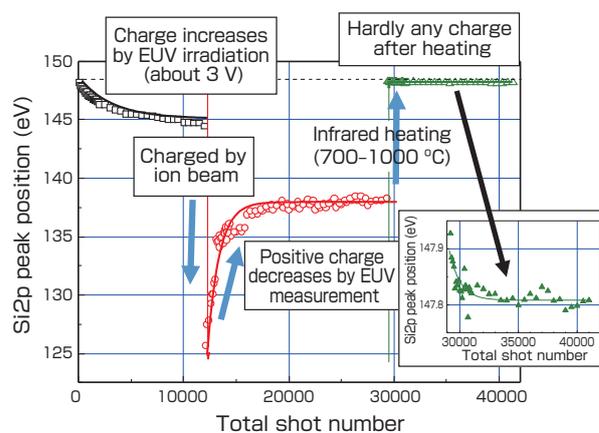
Fig. 13 Experiment that broke the "common sense" of photoelectron spectroscopy world that the thin insulator becomes charged because electrons go out of a sample
The amount of shift for SiO_2 of thickness of 100 nm charged positively with ion gun decreased by EUV measurement. This is thought to occur as the sample gained photoconductivity through EUV irradiation.

and the stored charges are released. It is thought that a similar phenomenon occurs in the XPS and the electron microscope, but we believe we are the first to make the argument that the insulating film becomes conductive during actinic excitation.

From fig.13, we can say that the charge shift of an insulating film is determined by the number of charge traps from the following three reasons: first, the large charge shifts generated by ion irradiation decreased rapidly by EUV irradiation but stopped at about 10-eV shift; second, the charge shift disappeared completely by infrared heating and annealing; and third, while the charge shift by EUV irradiation was 3-eV initially, it was only 0.1-eV after high-temperature annealing. The number of charge traps can be said to be as follows: after ion irradiation > initial stage > after high-temperature annealing.

We can say that the size of the charge shift is very important information of an insulator thin film, that is, the number of charge traps, and it should not be lost by neutralization.

5.4 Evaluation of electric conductivity from the charge shift

The insulating material with thickness over 1-μm such as a glass plate does not allow EUV light to pass through, therefore, will not become conductive with EUV irradiation. A thick insulator is charged as the electrons are released in the vacuum by EUV irradiation.

One user once asked us to analyze catalysts. When powder catalysts were measured at room temperature, there were absolutely no spectrum structure due to a very large charge shift, and the spectrum structure gradually appeared when the temperature was increased. When the temperature was increased further, the peak position shifted to the high kinetic energy side. This told us that the charge shift was smaller for higher temperature. The temperature dependence of the charge shift was different for different catalysts. The results are shown in Fig. 14.
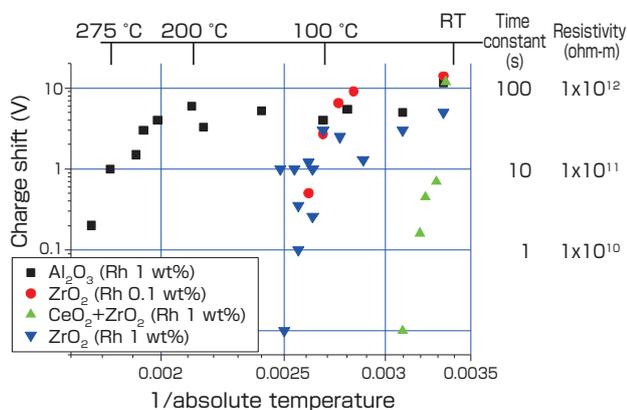
The charge shift can be related to electric conductivity.

When the sample with thickness d and a surface area S is replaced with an electric circuit with capacitance C and leak resistance R, the charge Q on the surface decreases with time constant $\tau = CR$. Since C and R can be expressed by $C = \varepsilon S/d$ and $R = \rho d/S$, using electric conductivity ρ and permittivity ε, it is $\tau = CR = \varepsilon \rho$. That is, time constant τ of discharge is not dependent on the shape of the sample (S and d). The permittivity is only several times different for different materials, and it does not differ greatly in the same material at different temperatures. On the other hand, conductivity changes by several orders of magnitude. Therefore, the discharge time constant gives electric conductivity.

In photoelectron spectroscopy, the peak shift occurs (Fig. 15) by the positive charge remaining in a sample after electrons are released into the vacuum. The positive charge is accumulated when the excitation continues. But accumulated charges leak with time constant τ. Then, the amount of accumulated charge becomes saturated with time constant τ. If the size of the charge shift in one shot is set as V_0 and the pulse interval as ΔT, the shift V after n shots is given by

$$V = V_0(1-\exp(-\Delta T/\Delta))^n/(1-\exp(-\Delta T/\tau))$$

and the saturation value ($\fallingdotseq V_0(\tau/\Delta T)$) is proportional to the time constant τ. The size of the charge shift V_0 in one shot is dependent on the pulse energy and C that is determined by the shape of the sample. The time constant is given from the charge shift when calibration is done. Then, when the permittivity is known, the absolute value of the electric conductivity is given.

This method has the advantage that it can be applied to materials with all sorts of shapes including fine particles. It is now used as a method in the research of correlation between catalyst activity and conductivity of powder catalysts.[31]

Fig. 14 Correlation was seen in the catalyst activity and the electric conductivity estimated from charge shift
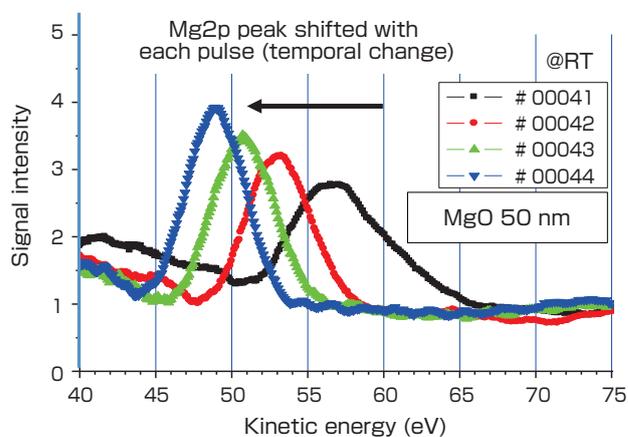
Fig. 15 Mg2p peak of MgO of thickness 50-nm shifted with every measurement
Electric conductivity is calculated from the time constant of shift.

5.5 Measurement of secondary electrons started by request from users

The measurement of secondary electrons was started by the request from the researchers of Panasonic Corporation who conducted the analysis of protection insulating film of electrodes in a plasma display using EUPS. They wanted to see the change of the vacuum level of the film by contamination. To answer their request, we improved the structures of the manipulator and the sample holder of EUPS so that we could control the potential of the sample.

5.5.1 Evaluation of the vacuum level (work function)

Primary electrons ejected out of atoms after gaining energy from photons collide with surrounding atoms, kick out new electrons (secondary electrons) from these atoms, and slightly lose energy. The primary electrons continue to collide with the surrounding atoms, kick out more secondary electrons, and continue to lose energy. Likewise, the secondary electrons collide with surrounding atoms and produce new secondary electrons. A large number of secondary electrons are produced like an avalanche, and the sea of secondary electrons is formed in the sample. The secondary electrons with kinetic energy surpassing the vacuum level are detected. Therefore, the vacuum level is obtained from the cutoff position of the energy spectrum of the secondary electrons.

An example of secondary electron spectra for TaN and W films with thickness of 10-nm formed on a Si wafer are shown in Fig. 16. In the case of TaN film, there is a sharp edge at 2.6-eV, and in the case of W, the sharp edge is at 3.5-eV. From these, it is found that the vacuum level of W was 0.9-eV higher than the vacuum level of TaN, and that the presence or absence of SiO_2 between the substrates did not change the vacuum level.[32]

Trajectories of electrons with small kinetic energy are easily affected by a very small floating electric field or magnetic field in the space around a sample, and the fraction arriving at the detector can be affected. To avoid this, the measurement of secondary electrons is performed by applying a negative potential bias to the sample holder to accelerate the electrons. In Fig. 16, bias of −2 V was applied to the sample holder in the measurement.
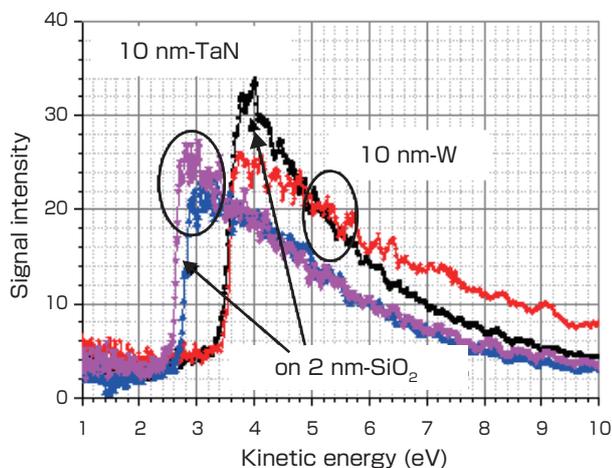
In the measurement of secondary electron spectra, it is often necessary to measure a wide range of several tens of eV with a very high energy resolution of several tens of meV. The TOF method is most powerful for such ultra-multi-channel measurements.

5.5.2 Evaluation of ultra-cleanliness of metal surface and evaluation of carrier density from secondary electron intensity

The above vacuum level observation was a response to the users' demand, but we realized that the intensity of the secondary electron was different for various samples (Fig. 17). Signals were small in metals and large in insulators. We interpreted this as meaning that the difference in the signal intensity of secondary electrons was due to the difference in the escape depth of low energy electrons.

In the case of insulating samples, new excitation of electrons cannot occur when the energy of the electrons becomes smaller than the band gap energy, and the electrons can reach the sample surface without losing any more energy and can escape into the vacuum.

On the other hand, for metals in which the Fermi level is in the continuous band, the electrons can be excited no matter how low the energy of the secondary electrons is, and electrons keep losing energy. Only the secondary electron that was created in the atom very close to the sample surface can escape to the vacuum. The escape depth of low energy electrons in metal is very small, and the secondary electron

Fig. 16 Secondary electron spectra of TaN and W of thickness 10 nm
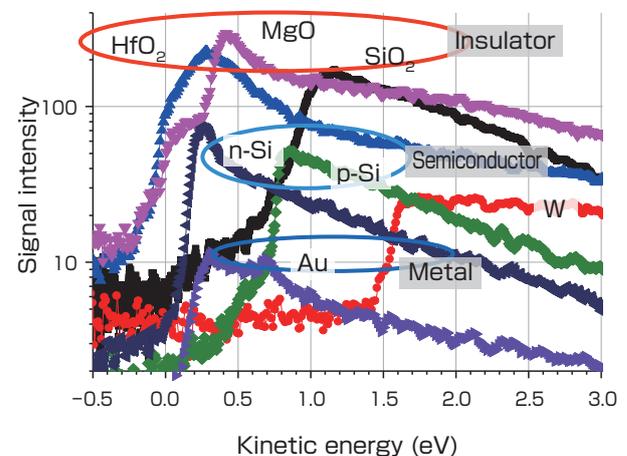
Fig. 17 Intensities of the secondary electron signals are in order of: insulator > semiconductor > metal

intensity of metal is small.

By knowing this principle, the metallic property of an ultrathin film or nm size particles can be evaluated, as shown in Fig. 18. Samples were TaN films with a different thickness formed on a W film of 100-nm thickness. Metal W has a weak secondary electron intensity and the effect of the transmission electrons from the underlying W layer is small. The secondary electron signal intensity was the smallest for a 10-nm TaN film, increased as the thickness decreased, and it was four times the intensity of 10-nm for TaN thickness of 1-nm. This result showed that the metallic property weakened as the film thickness decreased.[33]

This analysis method allowed a qualitative discussion of carrier density of organic semiconductor laser materials. By doping, the carrier density of organic semiconductor materials for optical devices is expected to increase, the resistance reduces, and enables injected current density to a higher level. The secondary electron spectrum of n-type AC5-CF$_3$ with 2 % Cs$_2$CO$_3$ as a dopant showed 0.9-eV lower cutoff position, and the signal intensity was half of that of a non-doped sample. This showed that doping lifts the Fermi level up by 0.9-eV against the vacuum level, and increases the carrier density. Incidentally, the secondary electron intensity of AC5 that had 1-eV greater work function compared to AC5-CF$_3$ was twice that of AC5-CF$_3$.[34][35]

5.6 Correlation between the inclination angle of electron clouds and catalyst activities

Emission from LPP is non-polarized, but in EUPS Unit 2, the measurement is the same as the polarized excitation owing to its configuration. EUV light irradiates sample horizontally and the electrons are detected at the vertical direction, and therefore, the electrons shaken in the electric field that oscillates horizontally (s polarization) are not detected, and only the electrons vertically shaken by p polarization are detected. Therefore, the angular distribution of the electron cloud can be observed from the angular dependence of the spectrum intensity by changing the angle of the sample (Fig. 19).
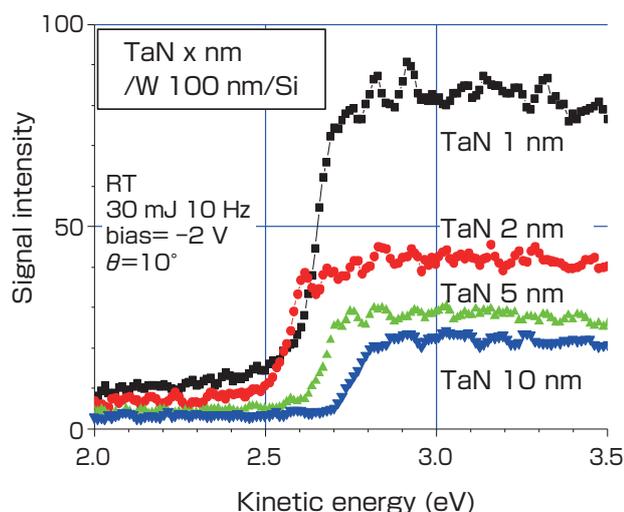
The angular distribution of the electron cloud was detected for the first time in a Si wafer. The direction of Si3p differed for different crystal orientation.

We were greatly surprised when we observed the angular dependence in the photoelectron spectrum of a powder sample that will be mentioned later. The direction of the electron cloud is usually considered to be determined by the crystal plane. If that is the case, the angular dependence should disappear in a powder sample in which crystal planes of individual particles are randomly oriented. Yet, there was angular dependence in powder samples. This means that the direction of the electron cloud is determined by the exterior form rather than the crystal plane, and this is extremely interesting. This phenomenon occurs only for the topmost atoms, and cannot be observed by XPS which gives information averaged over several nm depth.

ZrO$_2$ powder is employed as a catalyst for cleaning automobile exhaust gas. We measured the Zr3d photoelectron peaks of seven types of ZrO$_2$ powder samples with different additive precious metals. We found that the angles at the maximum intensity were different for different catalysts, and extremely good correlation was seen between the angle and the catalyst activity of water gas shift reaction of CO + H$_2$O $\leftrightarrows$ CO$_2$ + H$_2$.[36] It is probably the first time that the correlation between the efficiency of dissolution of gas molecules and the inclination angle of the electron clouds of catalyst atoms was found. It is expected to provide important information for the understanding of the catalyst mechanism. This analysis is unique to EUPS which sees the topmost atomic layer.

Fig. 18 Secondary electron spectrum of the TaN ultrathin film[32]

Since the signal is larger for thinner TaN, it can be said that the TaN film has lower electron density as it gets thinner.
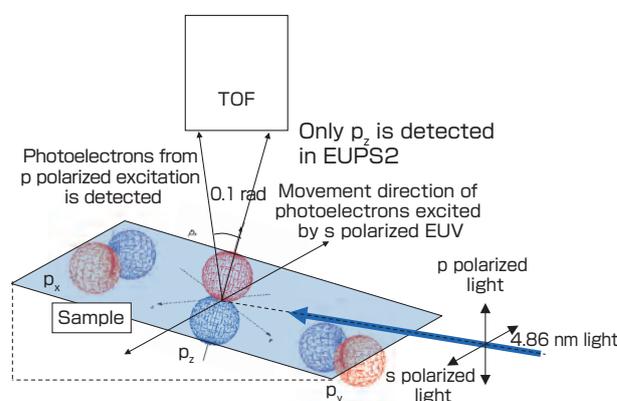
Fig. 19 In EUPS Unit 2, the electrons excited by p polarization of horizontal irradiation are detected by the detector installed vertically

5.7 Observation of the conduction band and the intra-gap states[Term 7]

Figure 20 shows the photoelectron spectrum near the Fermi level for four samples. As mentioned in Subchapter 4.6, we conducted improvements recently to enable obtaining event count data using the oscilloscope in the sequential mode. Therefore, it became possible to observe an extremely weak structure. Thus, it became possible to remove the effect of continuous spectra in the light source. By looking at Fig. 4 carefully, readers will notice that the 4.86-nm line emission lies on a weak continuous spectrum. The contribution of the continuum component was ignored until now because it was very small and was not easy to estimate. The contribution can be estimated by observing the sharp structure of the Fermi edge. Figure 20 is the spectrum after removing the effect of the continuous spectra. The signal intensity of four samples were different, and spectra were normalized at the peak.

As seen in the left figure of Fig. 20, sharp Fermi edges can be seen in the d band for Pt and Pd. As seen in the graph on the right that is the expanded vertical axis of the graph on the left, signals of 1–2 % intensity of the peak were seen at the energy above the Fermi level.

In the SiO_2 with thickness of 100-nm, there was a flat structure of about 2 % of the peak in the energy region between the Fermi level and the valence band top that dropped sharply at 5-eV below the Fermi level which lies at the 22-eV position of the horizontal axis. In the case of HfO_2 formed on 100-nm SiO_2, the signal near the Fermi level was large to the extent that the valence band top was not clear.

Since the size and spectral form were different for samples, the observed conduction band electron signal is considered real, but since the signal is weak, further research is necessary to be confident that it is real.

The lifetime of conduction band electrons in bulk metal is reported to be <1 fs–100 fs.[37] However, the lifetime of the surface states can be fairly long. In EUPS in which a sample is excited by ultrahigh density excitation of 3-ns pulse, it is no mystery if the transient states is observed. It is thought that the conduction band states and the intra-gap states at the surface-interface have large effect on properties of materials, and their analyses are important.

6 Summary

The characteristics of an LPP source are a narrow bandwidth line emission, a short pulse, and high brilliance. EUPS is an application taking full advantage of LPP. This is probably the first commercially viable technology of LPP application. The basic important synthesis technology is to obtain narrowband light without using a spectrometer and conducting the electron energy analysis by the TOF method. However, development of many elemental technologies was necessary before materialization of the basic idea. In this paper, we explained the process of synthesis to make the spectroscopy system as a working apparatus.

The shielding of contaminants, the greatest issue of LPP source applications, was solved using a BN rod as an LPP production target and an inexpensive Mylar film as the filter to block contamination. The frequent exchange of the shielding filter was reduced greatly by the introduction of an elliptical mirror. By not inserting a diffraction grating, the time averaged flux on a sample of EUPS is comparable to that using synchrotron radiation. The TOF method was employed as the electron energy analysis by taking advantage of the pulse nature of an LPP source. Problems of TOF not imagined when the basic principle was born arose when the actual measurements were conducted. The problems were solved by improving the structure of the flight tube.
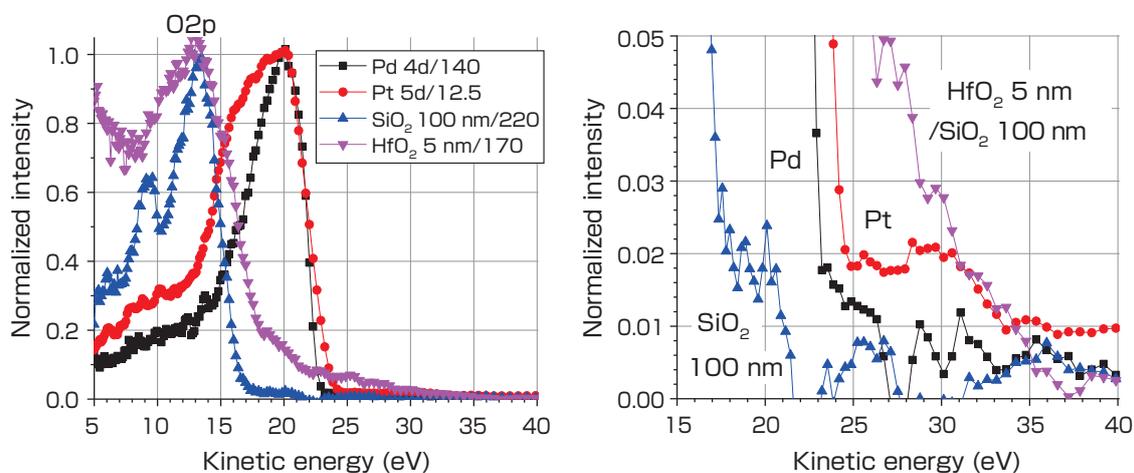
Fig. 20 Photoelectron spectra near the Fermi level for Pd, Pt, SiO_2, and HfO_2
Normalized by the peak signal. In the right graph that is the enlarged portion of the vertical axis of the left graph, the conduction band signals with intensity around 1 % of the peak are observed.

When the actual measurements of samples began, unexpected phenomena occurred one after another. By understanding them one by one, new analysis methods that could not be done with the conventional photoelectron spectroscopy were born. These include the detection of less than one monolayer contamination on material surface, detection of defects, measurement of insulator thin films without charge neutralization, evaluation of electric conductivity using the charge shift, observation of inclination angle of the electron cloud of the topmost atom, evaluation of electron density near the Fermi level from the secondary electron signal intensity, evaluation of the ultra-cleanliness of the surface of nm -size metal particles, and others.

The EUPS system was completed when the authors belonged to the Advanced Semiconductor Research Center, and since we know many researchers studying semiconductors, measurements were done mainly for semiconductor samples at the time. Due to the appearance of enthusiastic external users, the majority of the measurements are now for samples other than semiconductors. Since EUPS provides various findings for the topmost atom, it is expected to be most productive in the analysis of the catalytic phenomenon for which reactions occur at the topmost layer of atoms. In fields other than catalysts, if it is known that the topmost atom plays a critical role, EUPS will also be effective in that field. To expand to such new fields, participation of diverse users is necessary. Many of the new analysis methods unique to EUPS were born from the analyses of samples brought in by users. The author who started EUPS development without experience in photoelectron spectroscopy could not imagine the new ways of applying photoelectron spectroscopy and the wonderful potential of EUPS was made clear by enthusiastic users. I think "users' demand advances the device" is a principle that is widely applicable.

In terms of user-friendliness, EUPS does not compare with the XPS or UPS that are widely employed photoelectron spectroscopy. Drastic improvement of user-friendliness cannot be resolved by the author alone, and wide diffusion of EUPS analysis is necessary upon product realization. However, I think it is the responsibility and obligation of the inventor to bring EUPS to product realization.

Acknowledgements

Footnotes

Footnote 1. Mechanism of X-ray production from LPP: When free electrons are captured by fully ionized boron ion, and when the main quantum number transition from n=2 to n=1 occurs, 4.86-nm Lyman α ray is emitted. In EUPS, the laser focusing density is adjusted to get an appropriate temperature at which the fully ionized boron ions will be present in sufficient amount, and at which the free electrons recombine at sufficiently high speed. The emission intensity is proportional to the product of ion density and electron density, that is, the square of plasma density, and the emission intensity increases as the plasma density is higher. On the other hand, if the density is too high, self-absorption increases, intensity is saturated, and the width of the line spectrum broadens. The limit intensity is the intensity of "blackbody radiation," and at extremely high density, the spectral structures disappear and a spectral structure becomes flat. In EUPS, since the spectral width of excited EUV is determined by the emission spectrum of LPP, the plasma density should not be too

Hydrogen-like boron ion
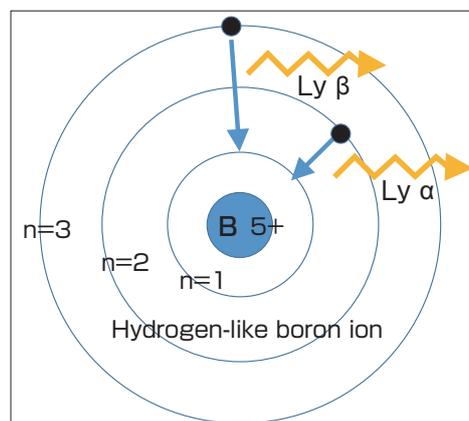
high. On the other hand, since strong emission is desired, some degree of density is wanted. The density of LPP depends on the wavelength of the excitation laser. The second harmonic of YAG laser with wavelength of 0.53-µm is an appropriate wavelength for producing narrow bandwidth of 4.86-nm light.

Footnote 2. Difference between LPPs for lithography and photoelectron spectroscopy: The requirements for light sources differ greatly for photoelectron spectroscopy and lithography. For the EUVL source, the requirements include high EUV power, low fluctuation of power, high conversion efficiency from lasers to EUV power, and being maintenance free for a long period such as one year. On the other hand, for the photoelectron spectroscopy source, narrow spectral width is the most important. Small power fluctuation, high conversion efficiency, and maintenance free characteristics are desirable, but they are not critical requirements. In EUPS, narrow bandwidth is a critical requirement to the LPP emission since a spectrometer is not used. For the EUVL source, wide emission that covers all widths (about 2 %) of the multilayer film reflection spectrum is needed to increase the usable power, but for EUPS, narrow bandwidth emission of about 0.1 % is required. In the TOF method, since the energy resolution is determined by time resolution, the emission time of the source is desired to be as short as possible, and it is 3-ns in the present EUPS. On the other hand, for the lithography source, the pulse width should be as wide as possible to have large power.[38] Pulse width of several tens ns is used. Therefore, all things are different for lithography and EUPS sources, including the laser selection, irradiation conditions, target materials, structures, and supply methods. For the target material, Sn is used in EUVL, while BN is used for EUPS. Rod target is used in EUPS while liquid droplets are used in EUVL. In EUPS, a YAG laser with pulse width of 3-ns, a wavelength of 0.53-µm, and repetition rate of 10 Hz is used, while for EUVL, a YAG laser with a wavelength of 1-µm or a CO_2 laser with a wavelength of 10.6-µm is used. EUPS uses single pulses, but for the EUVL source, use of prepulses is mandatory. Totally different LPP sources are used in these two applications, and the development of light source technology in one area does not benefit the other.

Footnote 3. Comparison of EUPS and XPS: While the XPS analysis is essential in today's material development, taking a rather self-centered view, it is stuck in element analysis. An analysis that captures the attractive topmost phenomenon that delves into the essence of material functionality as described in this paper is not being done with XPS. However, since XPS can excite the deep inner shell and is highly effective for element analysis, EUPS will never replace XPS in that area. As the product realization technology for EUPS progresses, it is thought that the price of EUPS will become less expensive.

Terminologies

Term 1. Magnetic bottle: The arrangement of a magnetic force line in the form of a bottle. It is an idea that when a sample is placed at the mouth of the bottle with magnetic flux density of 1 tesla or more, and the electron is wound around the magnetic line and the line is adiabatically expanded, only the direction of motion is changed without changing the kinetic energy of the electron, and therefore the enlarged image of the electron can be obtained in the electron detector placed at the bottom position of the bottle. The reason we were unable to observe the expected performance might possibly be because the magnetic bottle used in Unit 3 did not have a sufficient performance level, and there is room for success in future development. However, to raise the magnetic flux density to 1 tesla or more, there is only 1 mm or less space available for the sample. Since we realized that this lack of space severely limited the samples that could be measured, we stopped the use of the magnetic bottle.

Term 2. Schwarzschild optics: To focus light onto minute diameters, it is necessary to decrease optical aberration, and near normal incidence is required. A Schwarzschild optics is a near normal incidence optical system that combines concave and convex mirrors, and submicron resolution can be achieved. However, it is not easy to obtain large vertical reflectivity in X-ray multilayer films, and the high normal incidence reflectivity of about 70 % has been obtained only for Mo/Si multilayer films. This is the reason 13.5 nm was selected in EUVL that uses more than ten multilayer mirrors.

Term 3. Microchannel plate (MCP): High-speed particle detector. About 2-kV of voltage is applied between both sides of a circular or rectangular glass plate where many microchannels of inner diameter of around 10-µm are bundled together. The secondary electrons produced at the MCP surface due to particle collision are led to the microchannels to achieve many orders of magnitude amplification. With a multiplication factor of 10^7 or more, the detection of a single electron becomes possible. It is characterized by high-speed response where the

start-up time is 1-ns or less, and this is essential in TOF electron spectroscopy.

Term 4. Stimulated Brillouin scattering (SBS) mirror: When reflected wave having reversed phase with the incidence wave (phase conjugation) is generated, the diffraction-grating-like sound waves are produced in a substance due to the interference of the two waves. In stimulated Brillouin scattering that is the back scatter of the laser light by a sound wave, the wave front distortion of the incident wave that experiences as it passes through a distorted laser gain medium and the wave front distortion of the reflected waves are in antiphase. Therefore, the wave front distortion of the returning laser beam does not increase when the laser beam goes back and forth in the laser medium having a large optical distortion caused by strong excitation. Thus, good quality laser beam is obtained with a SBS mirror.

Term 5. Semiconductor doping: The Fermi level, which is the energy level at which the probability that electron exists is 50 %, is the center of the band gap in non-doped semiconductors. Impurities are introduced (doping) to adjust the position of the Fermi level to control the height of the Schottky barrier. When doping is done with impurities that supply electrons, the Fermi level approaches the bottom of the conduction band and an n-type semiconductor is formed, and when doping is done with impurities that receive electrons, a p-type semiconductor is formed.

Term 6. Band bending: Very often, the charge is captured in the interface, or the charge is captured in the insulating film that is sandwiched between the metal and the semiconductor, and the band position at the interface of the conduction band bottom of the semiconductor may be different from the position in the bulk. Then, the control of expected carrier transportation will be lost, and the device performance decreases. It is very important in device development to know the size of band bending and how to decrease unintended
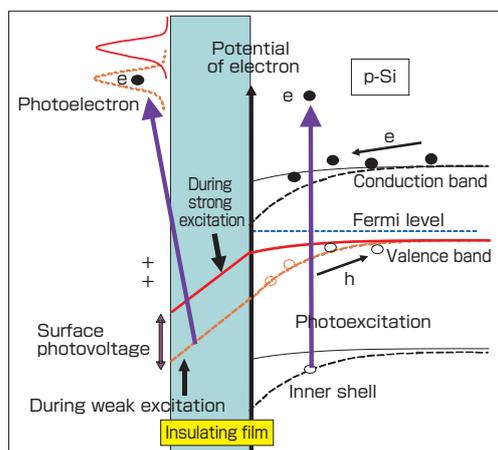
band bending. Since the flattening of the band is accomplished by strong excitation in EUPS, band bending can be evaluated from the difference of the positions of photoelectron spectra by changing excitation intensity.

Term 7. Intra-gap level: In crystals, energy gap is formed as the energy level separates into the valance band and the conduction band by periodicity. However, in surface interfaces, periodicity in the depth direction is lost, band boundaries become unclear, and electron levels occur in the energy position that corresponds to the energy gap of the bulk. Since this is thought to greatly affect the transportation property of the carrier, the evaluation of the position and the amount of intra-gap levels is important. Particularly, in catalysts where the reactions occur on the topmost atom, it is possible that the intra-gap level plays a definitive role in catalyst activity.

References

[1] "Kodenshi bunko hoho (Photoelectron spectroscopy)," Japan Patent No. 2580515 (1996) (in Japanese). "Denshi bunko hoho to kore o mochiita denshi bunko sochi (Electron spectroscopy and electron spectroscopy apparatus)," Japan Patent No. 2764505 (1998) (in Japanese). "Electron spectroscopy apparatus," US Patent No. 5569916 (1996).

[2] Nanotech Japan: http://nanonet.mext.go.jp/, accessed 2016-05-17 (in Japanese).

[3] T. H. Maiman: Stimulated optical radiation in ruby, *Nature*, 187, 493–494 (1960).

[4] J. Nuckolls, L. Wood, A. Thiessen and G. Zimmerman: Laser compression of matter to super-high densities: Thermonuclear (CTR) applications, *Nature*, 239, 139–142 (1972).

[5] T. Tomie: Picosecond pulse generation by self-phase modulation in an actively mode-locked and Q-switched phosphate glass laser, *Jpn. J. Appl. Phys.*, 24, 1008–1017 (1985).

[6] P. Langer, G. Tonon, F. Floux and A. Dugauze: Laser induced emission of electrons, ions, and X rays from solid targets, *IEEE J. Quantum, Electr.*, 2 (9), 499–506 (1966).

[7] M. J. Bernstein and G. G. Comisar: X-ray production in laser-heated plasmas, *J. Appl. Phys.*, 41, 729–733 (1970).

[8] D. L. Spears and H. I. Smith: X-ray lithography: A new high resolution replication process, *Solid State Technol.*, 15 (7), 21–26 (1972).

[9] T. Tomie, H. Shimizu, T. Majima, T. Kanayama, M. Yamada and E. Miura: Flash contact x-ray microscopy of biological specimen in water, *Proc. SPIE*, 1741, (1993).

[10] T. Tomie, H. Kondo and H. Shimizu: Application of X-ray laser to photoelectron micro-spectroscopy, *Inst. Phys. Conf.*, 151, 520–527 (1996).

[11] T. Tomie, H. Shimizu, T. Majima, M. Yamada, T. Kanayama, H. Kondo, M. Yano and M. Ono: Three-dimensional readout of flash x-ray images of living sperm in water by atomic-force microscopy, *Science*, 252, 691–693 (1991).

[12] L. I. Gudzenko and L. A. Shelepin: Negative absorption in a nonequilibrium hydrogen plasma, *Sov. Phys. JETP*, 18, 998–1000 (1964).

[13] A. G. Molchanov: Lasers in the vacuum ultraviolet and in

the x-ray regions of the spectrum, *Sov. Phys. Usp.*, 15, 124–129 (1972).

[14] C. Chenais-Popovics, R. Corbett, C. J. Hooker, M. H. Key, G. P. Kiehn, C. L. S. Lewis, G. J. Pert, C. Regan, S. J. Rose, S. Sadaat, R. Smith, T. Tomie and O. Willi: Laser amplification at 18.2 nm in recombining plasma from a laser-irradiated carbon fiber, *Phys. Rev. Lett.*, 59 (19), 2161–2165 (1987).

[15] M. Grande, M. H. Key, G. Kiehn, C. L. S. Lewis, G. J. Pert, S. A. Ramsden, C. Regan, S. J. Rose, R. Smith, T. Tomie and O. Willi: Measurement and detailed analysis of single pass gain at 81 Å in a recombining laser produced fluorine plasma, *Opt. Commun.*, 74, 309–312 (1990).

[16] R. London, D. Matthews and S. Suckewer (eds.): *Proc. Applications of X-ray Lasers* (1992).

[17] T. Tomie: Tin laser-produced plasma as the light source for extreme ultraviolet lithography high-volume manufacturing: History, ideal plasma, present status, and prospects, *J. Micro/Nanolith. MEMS MOEMS*, 11 (2), 021109 (2012).

[18] T. Tomie, H. Kondo, H. Shimizu and P. Lu: X-ray photoelectron spectroscopy with a laser plasma source, *Proc. SPIE*, 3157, 176–183 (1997).

[19] S. Aoki, T. Ohchi, S. Sudo, K. Nakajima, T. Onuki and K. Sugisaki: X-ray photoelectron spectroscopy using a focused-laser-produced plasma x-ray beam, *Jpn. J. Appl. Phys.*, 32, L1574–1576 (1993).

[20] T. Munakata, E. Ishikawa, I. Kinoshita and T. Kasuya: Scanning photoelectron spectromicroscope based on coherent vacuum ultraviolet radiation, *Rev. Sci. Instrum.*, 62, 2572–2578 (1991).

[21] H. Kondo, T. Tomie and H. Shimizu: Time of flight photoelectron spectroscopy with a laser-plasma x-ray source, *Appl. Phys. Lett.*, 69 (2), 182–184 (1996).

[22] H. Kondo, T. Tomie and H. Shimizu: Observation of chemical shifts of Si 2p level by an x-ray photoelectron spectroscopy with a laser-plasma x-ray source, *Appl. Phys. Lett.*, 72 (21), 2668–2670 (1998).

[23] Hikojikan-gata bunseki sochi (Time-of-flight analysis device), Japan Patent No. 4431698 (2010) (in Japanese).

[24] Hikojikan-gata energy bunko sochi (Time-of-flight energy spectroscopy device), Japan Patent No. 4936375 (2012) (in Japanese).

[25] T. Tomie, T. Ishitsuka, T. Ootsuka and H. Ota: Observation of work functions, metallicity, band bending, interfacial dipoles by EUPS for characterizing high-k/metal interfaces, *AIP Conf. Proc.*, 1395 (1), 148 (2011).

[26] Y. Morita, M. Terauchi, T. Nakayama, K. Yoshino, Y. Yamauchi and M. Nishitani: Characterization of protective layer materials for plasma display panel, *Monthly Display*, 12, 62 (2011) (in Japanese).

[27] M. P. Seah and W. A. Dench: Quantitative electron spectroscopy of surfaces: A standard data base for electron inelastic mean free paths in solids, *Surf. Interface Anal.*, 1 (1), 2–11 (1979).

[28] T. Ishitsuka, T. Ootsuka, T. Kasai, H. Ota and T. Tomie: Evaluation of inelastic mean free path of several eV electrons in metals by EUPS, 57th Spring Meeting of the Japan Society of Applied Physics, Kanagawa Institute of Technology, 25p-KW-7 (2011) (in Japanese).

[29] T. Tomie, T. Kasai, H. Iwazumi, T. Katayama, M. Inoue and K. Asayama: EUPS de sokutei shita HfSiON/Si no band magari no makuatsu izonsei (Dependency on film thickness dependency of the band bending of HfSiON/Si measured by EUPS), 54th Meeting of the Japan Society of Applied Physics, Aoyama Gakuin University), 28p-ZH-2 (2007) (in Japanese).

[30] T. Ootsuka, T. Ishitsuka, T. Kasai, Y. Morita, N. Hata and T. Tomie: Evaluation of thickness dependence of metallic property of TaN thin films by EUPS, 71st Autumn Meeting of the Japan Society of Applied Physics, Nagasaki University, 16p-S-17 (2010) (in Japanese).

[31] M. Nagata, T. Yamada, R. Ando, I. Kim and T. Tomie: Surface conductivity measurement of catalyst materials by EUPS and its correlation to catalyst performance, *SAE Int. J. Engines*, 9 (3), (2016).

[32] T. Ootsuka, T. Ishitsuka, T. Kasai, H. Ota and T. Tomie: Evaluation of work functions of TaN and W thin films by EUPS, 57th Spring Meeting of the Japan Society of Applied Physics, Tokai University Shonan Campus, 19p-C-7 (2010) (in Japanese).

[33] T. Ishitsuka, T. Ootsuka, T. Kasai, H. Ota and T. Tomie: Evaluation of thickness dependence of metallic property of TaN thin films by EUPS, 57th Spring Meeting of the Japan Society of Applied Physics, Tokai University Shonan Campus, 19p-C-9 (2010) (in Japanese).

[34] Y. Kawaguchi, F. Sasaki, H. Mochizuki, T. Ishitsuka, T. Tomie, T. Ootsuka, S. Watanabe, Y. Shimoi, T. Yamao and S.Hotta: Electronic states of thiophene/phenylene co-oligomers: Extreme-ultra violet excited photoelectron spectroscopy observations and density functional theory calculations, *J. Appl. Phys.*, 113, 083710 (2013).

[35] F. Sasaki, Y. Kawaguchi, H. Mochizuki, S. Haraichi, T. Ishitsuka, T. Ootsuka, T. Tomie, S. Watanabe, Y. Shimoi, T. Yamao and S.Hotta: Effects of pn doping in thiophene/phenylene co-oligomers thin films, *Mol. Cryst. Liq. Cryst.*, 620 (1), 153–158 (2015).

[36] T. Ishitsuka, T. Ito, M. Nagata and T. Tomie: Correlation of tilt angle of electron cloud of top surface atoms observed by EUPS with catalytic activity of powder catalysts for mobile exhaust, 57th Spring Meeting of the Japan Society of Applied Physics, Tokai University Shonan Campus, 18p-P-14 (2010) (in Japanese).

[37] M. Bauer and M. Aeschlimann: Dynamics of excited electrons in metals, thin films and nanostructures, *J. Electr. Spectr. Rel. Phen.*, 124, 225–243 (2002).

[38] T. Aota and T. Tomie: Ultimate efficiency of extreme ultraviolet radiation from a laser-produced plasma, *Phys. Rev. Lett.*, 94, 015004, (2005).

Authors

Toshihisa TOMIE
Engaged in the research of high-energy glass laser technology, X-ray microscopy, X-ray laser, photoelectron spectroscopy, EUVL source, and others at the Electrotechnical Laboratory and AIST. Visiting Researcher, Rutherford Appleton Laboratory of UK under Long-term Study Abroad Program for Nuclear Science of the Agency of Science and Technology in 1986. Invented the EUPS, X-ray refractive lens, defects inspection method of multilayer mask blank, and others. Has worked as Research Consultant, AIST; Program Manager, NEDO; and Visiting Researcher, AIST. Selected as one of foreign experts in the "1,000 Talent Plan" of the People's Republic of China and was appointed Special Professor at Changchun University of Science and Technology for three years starting July 2014. Awarded the title "State Specially Recruited Experts" in April 2014. Instructing the research

on EUV source and the research on the carrier dynamics in the Au-TiO$_2$ nanoparticle system using the photoelectron microscope PEEM and femto-second laser. Continues the EUPS research as a Visiting Researcher at AIST. In this paper, he was in charge of the invention of EUPS, the development of technologies for practical device, and the pioneering of new applications for photoelectron spectroscopy.

Tomoaki ISHITSUKA
Completed the master's course at the Graduate School of Science and Engineering, Ibaraki University in 1992. Joined Hitachi Maxell, Ltd. in 1992. Technical staff at AIST in 2008. Since then, has continuously worked on EUPS measurement. Currently engages in the R&D for EUPS and other devices and the support of projects using such devices (including the Microstructural Characterization Platform Project). In this paper, he was in charge of the measurement of most of data presented in Chapter 5.

Discussions with Reviewers

1 Overall
Comment (Naoto Kobayashi, Waseda University)

This is a paper on the development of the photoelectron spectroscopy method for the practical use of laser-produced plasma (LPP) and its various applications, for which the authors have engaged passionately in R&D. It explains the detailed course in which the initial objective for the LPP source was set, how the new photoelectron spectroscopy was gradually established, and how the technologies were put to various advanced applications, and I think the paper is valuable from scientific and engineering perspectives. This was a typical "seeds-driven" or potential-driven research that utilized the characteristics and advantages of the technological potential of the LPP source and achieved practical use, and you describe that the voices of various users played an important role in exploring various applications. The unique technological synthesis method and process make this a paper appropriate for publication in *Synthesiology*.

Comment (Ken'ichi Fujii, AIST)

While the X-ray photoelectron spectroscopy (XPS) is used widely for the analysis of the surface and its contamination state, the authors looked at the pulse laser produced plasma as the source for the XPS and went on to develop the extreme ultraviolet excited photoelectron spectroscopy (EUPS) along with its effective applications. I think the paper that records this process is extremely valuable.

Answer (Toshihisa Tomie)

We received your useful comments on this paper after you read it carefully. I believe your comments are appropriate. I also made some improvements on the structure of the paper, as you proposed, like adding explanations of terminologies at the end. The subtitle you proposed is attractive, and I shall use it.

2 LPP source
Comment (Ken'ichi Fujii)

To make this technology be known widely by general engineers and researchers, I think you need to offer a more understandable explanation on the production principle of the EUV light source. You have some explanation in Subchapter 1.2 "History of the research of laser-produced plasma source," but I think the reader's understanding will deepen if you explain, along with figures, what is the excitation laser used in LPP, and by what mechanism extreme ultraviolet light is produced.

Answer (Toshihisa Tomie)

The selection of the laser is important, and I listed the following requirements in Subchapter 4.4 "Selection of a laser." That is, the pulse waveform needs to be fine Gaussian with pulse width of 3 ns using stimulated Brillouin scattering (SBS) mirrors, the spatial pattern ought to be TEM00 mode, the good beam pattern and the pulse waveform ought to be obtained independent of the pulse energy and the repetition rate up to the repetition rate of 100 Hz, and others. As you proposed, I added some footnotes at the end of the text.

3 Future prospect
Comment (Naoto Kobayashi)

It can be seen that the newly pioneered EUPS has provided new observation methods for various substance surfaces. Particularly, new findings never seen before have been obtained for the behavior of electrons on the topmost surface. To which science and technology fields do you expect this technology will be applied in the future?

Answer (Toshihisa Tomie)

I added the following expression in Chapter 6 "Summary."

"Since EUPS provides various findings pertaining to the topmost atom, we believe it will be most effective in analyzing the catalyst phenomenon where the reaction occurs at the topmost surface of atoms."

4 Commercial device
Comment (Naoto Kobayashi)

The technology was advanced through many users, and I feel that some manufacturers will be interested in making a commercial device. Was there any such plan? If the prospect for that is not good, what are the barriers that stand before commercialization?

Answer (Toshihisa Tomie)

Ten years ago, I visited many analysis companies but their responses were not very good. Recently, many users have asked how much would it cost to manufacture a device, and some have commented that 50 million yen isn't that expensive, but no actual project has taken off.

Since the Panasonic Corporation, who improved the manufacturing process by EUPS analysis, withdrew from the plasma display panel business, we can no longer ask them to advertise our work. However, if we gain more case studies where people have been able to advance the business because they used the EUPS analysis, stories will circulate, and I think the demand for product realization will be strengthened. Before talking about product realization, the greatest reason the product has not gained awareness is the lack of basic data published in the scientific journals, and for this, we are totally guilty. Recently, there are papers written by users, and I hope the knowledge of this technology will gradually increase. I hope the commercialization will become more specific. As I wrote in Chapter 6 "Summary," it is my responsibility to work on EUPS until product realization.